IEEE Photonics Journal
An IEEE Photonics Society Publication

Open Access

Optically Pumped Hybrid Plasmonic-Photonic Waveguide Modulator Using the VO_2 Metal-Insulator Phase Transition

Volume 10, Number 1, February 2018

J. Kenji Clark
Ya-Lun Ho
Hiroaki Matsui
Jean-Jacques Delaunay

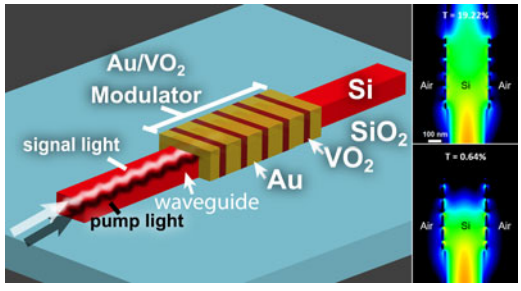

DOI: 10.1109/JPHOT.2017.2784429
1943-0655 © 2017 IEEE

Optically Pumped Hybrid Plasmonic-Photonic Waveguide Modulator Using the VO_2 Metal-Insulator Phase Transition

J. Kenji Clark,[1] Ya-Lun Ho,[1] Hiroaki Matsui,[2,3] and Jean-Jacques Delaunay [1]

[1]Department of Mechanical Engineering, The University of Tokyo, Tokyo 113-8654, Japan
[2]Department of Bioengineering, The University of Tokyo, Tokyo 113-8654, Japan
[3]Department of Electrical Engineering and Information Systems, The University of Tokyo, Tokyo 113-8654, Japan

DOI:10.1109/JPHOT.2017.2784429

Manuscript received September 18, 2017; revised December 7, 2017; accepted December 12, 2017. Date of publication December 18, 2017; date of current version January 3, 2018. This work was supported in part by the Japan Society for the Promotion of Science (JSPS) KAKENHI under Grants 17H03229 and 17K18867, and in part by the JSPS Core-to-Core Program (Advanced Research Networks type A). Corresponding author: J.-J. Delaunay (e-mail: jean@mech.t.u-tokyo.ac.jp).

Abstract: The need for ever faster and more efficient computation and communication devices has spurred interest in the field of all-optical modulators. Here a small-size hybrid plasmonic-photonic all-optical waveguide modulator utilizing a subwavelength Au/VO_2 nanostructure is proposed as a high-modulation optically actuatable modulator. Using finite-difference-time-domain simulations, a nanoscale (320 nm $\times$ 300 nm cross-section) optimized modulator is designed. The modulator design has an extinction ratio as high as 26.85 dB/μm, and a length of only 550 nm.

Index Terms: Nanophotonics, optical waveguides, plasmons.

1. Introduction

Year after year, as the density of transistors in microchips increases, the power consumed and heat generated by microchips increases. Ultimately, this limits the speed of these devices, and represents a bottleneck in the processing power of computational devices. Integrated optical devices could help alleviate some of these problems by providing low-loss and large bandwidth optical interconnects [1]. Their realization however, requires the development of optical modulators [1]. In recent years, a large amount of work has been dedicated to the demonstration of high efficiency optical modulators, with many different phenomena being used, including carrier depletion in silicon-waveguide modulators [2], optical pumping induced Pauli blocking in graphene [3], and thermally, electrically and optically induced phase changes and metal-insulator transitions [4]–[11]. A promising metal-insulator transition material for high-speed, small-size optical modulators is vanadium dioxide (VO_2).

VO_2 is a correlated oxide that can undergo a phase transition from a monoclinic insulator phase to a rutile metallic phase [12]. The metal-insulator transition phenomenon was first discovered to be thermally induced above 340 K [12]. However, since that time a variety of other means

have been shown to be capable of inducing the phase transition, including the application of an electrical bias [13], excitation by a terahertz wave [14] and hot-electron injection [15]. Recently it has even been demonstrated that using an optical excitation, the VO_2 metal-insulator transition can be triggered at sub-ps timescales and can likely be used for reversible high-speed modulation of VO_2 [16]. Thermally switched [5], [17], and electrically switched [18], waveguide integrated modulators incorporating VO_2 have been proposed and developed. However, an all-optical modulator that uses the high-speed optically induced phase transition of VO_2 remains to be demonstrated.

In order to realize a low-threshold and small-size waveguide integrated all-optical VO_2 optical modulator, plasmonic nanostructures are extremely useful. Plasmonic nanostructures are metallic nanostructures that can confine and concentrate light to sub-wavelength dimensions [19]. Such nanostructures have been used not only to achieve optical modes with subwavelength effective wavelengths [19], but also to enhance the electric field intensity of incident light for improving light-matter interaction in non-linear materials [20], surface enhanced Raman scattering (SERS) [21], and many other fields. A recent article even demonstrated the use of plasmonic nanoantennas to assist in the light-induced phase transition of VO_2 [22].

In this work, we propose and optimize the design of a hybrid photonic-plasmonic all-optical modulator. The device is comprised of a thin sub-wavelength Au/VO_2 nanostructure that coats a silicon waveguide. This hybrid structure allows an optical pump signal propagating in the silicon waveguide to be concentrated into the VO_2 in order to switch the VO_2 phase, and provides a resonant photonic cavity that enhances the contrast between the transmission of the modulator in the dielectric VO_2 state and the metallic VO_2 state. This design has the potential to realize an all-optical modulator with an extinction ratio (ER) as high as 26.85 dB/μm, while only being 550 nm in length.

2. Design Process

As a first step to the development of a high-speed all-optical modulator, an overall device architecture had to be envisaged. This device architecture needed to fulfill three key requirements. The first requirement was that the device should be easy to integrate with CMOS devices and telecommunication devices, the second requirement was that the device should concentrate a pump signal into the VO_2 in order to facilitate an optically induced phase change, and the third requirement was that the structure should be an efficient waveguide for the signal wavelength. To fulfill the first and third requirements, a silicon waveguide, designed for 1550 nm light, was chosen as the base for the modulator.

The devised waveguide structure is illustrated in Fig. 1(a). At the base of the device, is a patterned silicon-on-insulator (SOI) wafer with a Si ridge waveguide designed for a 1550 nm signal light. On top of the Si ridge waveguide is a nanostructure coating of Au and VO_2 that can trap a pump light propagating through the silicon waveguide into the VO_2. The Au/VO_2 nanostructure coating was made sub-wavelength and periodic in order to provide an effective waveguide medium for the efficient propagation of the 1550 nm signal light. The possibility of creating an effective waveguide medium from a subwavelength nanostructure has been demonstrated in the literature for Si/Air [23], and in this work we have applied the same principle to an Au/VO_2 nanostructure in order to form an effective hybrid plasmonic-photonic waveguide.

In the proposed design, there are a large number of parameters that affect the performance of the modulator, including the VO_2 length (L_{VO2}), the Au length (L_{Au}), the number of periodic elements in the device (N), the total modulator length (L_M), and the waveguide width (w), height (h) and nanostructure coating thickness (t). The waveguide width and height were fixed at 320 nm and 300 nm respectively in order to ensure single mode operation with the electrical field polarization being primarily horizontal. The thickness of the coating was fixed at 20 nm as it is understood that optical pumping of VO_2 induces a complete metal-insulator transition in individual VO_2 grains [24], and a 20 nm thickness will ensure each VO_2 domain is comprised of only a single crystal grain. In order to better understand the physical processes governing the performance of the modulator device and the impact of the other parameters, a 2-dimensional analogue to the 3-dimensional

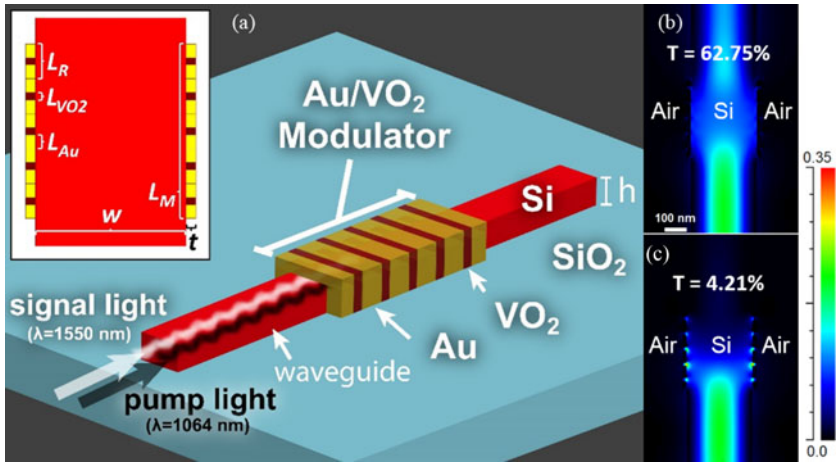

Fig. 1. Hybrid VO_2 all-optical modulator. (a) 3D waveguide structure, illustrating pump and signal light injection, (b, c) Poynting vector magnitude when VO_2 is (b) dielectric, and (c) metallic, for a 2D slab waveguide modulator.

waveguide was studied in detail and optimized in the following section. The impact of the VO_2 and Au ratio in the modulator, L_M, and L_R were studied and understood clearly based on the allowed photonic and plasmonic modes of the device. An ideal pump light wavelength was then determined. The Poynting vector magnitude and the transmission of the optimized 2D modulator when the VO_2 is in the dielectric state and metallic state are shown in Fig. 1(b) and (c) respectively. The ratio of the transmittance in the dielectric state (62.75%) to the transmittance in the metallic state (4.21%) corresponds to an ER (ratio of the transmittance in the on state to the transmittance in the off state) of 23.98 dB/μm. Finally, using the understanding developed from the study of the 2D simulation, a 3D simulation was designed and optimized.

The proposed nanostructure represents a CMOS compatible design that can be fabricated using standard nanofabrication procedures. Standard electron-beam lithography of an SOI wafer can be initially used to define the silicon waveguide. Following this, deposition of the VO_2, patterning with e-beam lithography and etching with reactive ion etching (RIE) can be done to create a sub-wavelength VO_2 grating. After this, Au deposition and lift-off of the gold can be performed to obtain the Au/VO_2 coated silicon waveguide. The possibility of achieving a high-quality sputtered film on the sidewalls of Si was demonstrated in previous work [25].

3. Optimization and Performance

3.1 Modal Analysis

A 2D optimization of the modulator structure was first performed in order to develop a clear understanding of the governing factors that determine the modulator performance. Simplifying the model to a 2D simulation makes the waveguide resonances much more evident. Before the proposed modulator structure could be optimized however, an understanding of how the optical modes propagate in the uncoated, Au coated and VO_2 coated waveguides needed to be developed. For this purpose, a modal analysis was performed using the finite-difference-time-domain technique (FullWAVE, Rsoft Design Group, Ossining, USA). The calculated mode indices and mode profiles for a 320 nm wide slab waveguide with no coating, an Au coating, a dielectric VO_2 coating and a metallic VO_2 coating are shown in Fig. 2. Refractive indices for the dielectric and metallic VO_2 states were taken from a previous article [26], and indices for Au [27], Si [28] and SiO_2 [29] were taken from the literature. For the uncoated silicon waveguide, and both the metallic phase and dielectric phase VO_2, the propagating modes are photonic modes with effective indices near the silicon

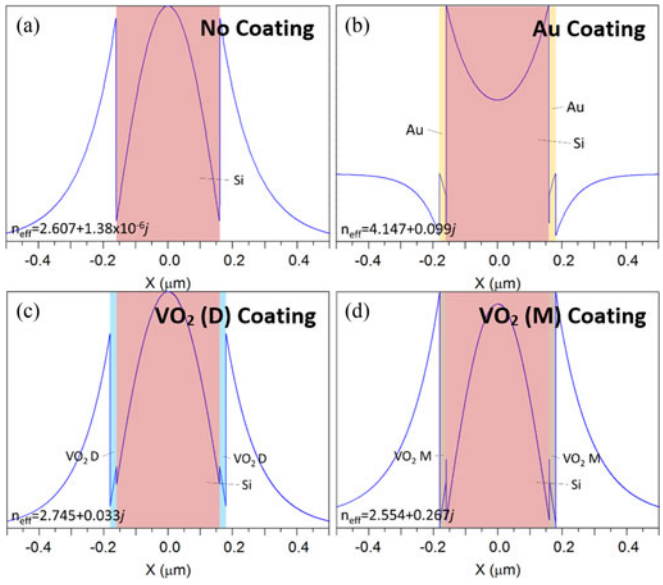

Fig. 2. The effective mode indices and modal field distributions of the TM_0 mode for a 320 nm wide silicon slab waveguide, with (a) no coating, (b) a 20 nm thick gold coating, (c) a 20 nm thick coating of VO_2 in the dielectric phase of VO_2, and (d) a 20 nm thick coating of VO_2 in the metallic phase of VO_2.

waveguide index of 2.607. The drastic difference between the imaginary component of the effective index for the metallic and dielectric VO_2 indicates that the mode is far more lossy in the metallic VO_2 case, which will result in a large contrast between the transmission of a metallic VO_2 coated waveguide and a dielectric VO_2 coated waveguide. It is evident from the electric field distribution of the Au coated silicon waveguide mode that the mode is a plasmonic metal-insulator-metal (MIM) waveguide mode with a high effective index. The high effective index is characteristic of plasmonic modes, and allows the device size to be reduced [30].

We subsequently demonstrated (see Fig. 3) that the waveguides described above can form resonant cavities that either enhance the transmission or reflection of the waveguide depending on the effective optical length of the waveguide. In the case of the Au coated waveguide, the calculated effective index was $4.147 + 0.099j$. Based on this value, the effective longitudinal wavelength for 1550 nm light within the waveguide is approximately 374 nm. It can be expected that light reflected from the ends of the waveguide will interfere with each other, and that the transmitted and reflected intensity (T and R respectively) will depend on the length of the waveguide. Where a minimum or maximum in the reflection of the waveguide is found, we expect another when L_M is $\lambda_{eff}/2$ longer, as this will correspond to an optical path length difference of λ_{eff}, where the optical phase must be the same. For the Au coated waveguide, we therefore expect that if the reflectance is plotted against the waveguide length [see Fig. 3(b)], the distance between two reflectance peaks should be approximately 187 nm. The value obtained in simulation was 185 ± 20 nm, and therefore fits this explanation. For the dielectric VO_2 coated waveguide [see Fig. 3(c)], the value predicted based on the effective index was 282 nm, and the value obtained in simulation was 270 ± 20 nm. For the metallic VO_2 coated waveguide [see Fig. 3(d)], the predicted value was 303 nm, and the obtained value was 295 ± 20 nm. These results clearly indicate that the modulator can act as a resonant cavity, for which the total length of the modulator is important in determining the transmissivity, and hence efficiency of the modulator.

This phenomenon was subsequently applied to the hybrid Au/VO_2 coated nanostructure in order to optimize the effective optical length of the entire modulator structure, and in doing so maximize the transmission when VO_2 is in its dielectric state, in order to obtain a high ER modulator.

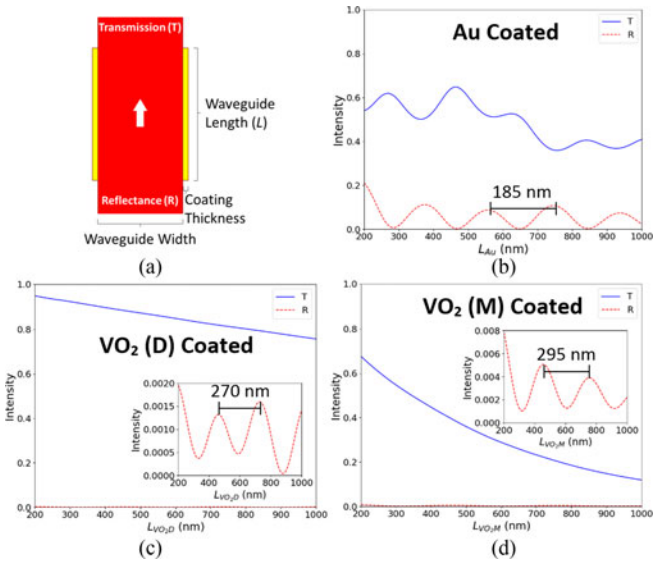

Fig. 3. (a) Illustration of the simulated 2D waveguide structure. Simulated reflectance and transmittance of waveguides composed of a silicon core and a thin film on either side of the silicon, where the thin film is (b) gold, (c) dielectric VO_2, or (d) metallic VO_2 are shown in (b), (c) and (d). Insets in (c) and (d) show reflectance.

3.2 2-D Optimization

In order to determine the ideal modulator parameters and understand the underlying physical principles of the device, we optimized three main parameters. The first parameter was the ratio of L_{Au} to L_{VO2} in the periodic element, the second was the number of periodic units in the modulator, and the final parameter was the length of the individual periodic units. Since the sub-wavelength periodic elements will behave as a single effective waveguide, the initial Au/VO_2 ratio optimization [see Fig. 4(b)] was performed in order to determine the ideal waveguide medium for the modulator. Although the ER will intuitively increase overall as the modulator length increases, it was expected that there would be an optimal length of the device for which a maximal ER per unit length would be achieved. To determine this length, the dependence of the ER per unit length on the number of periodic units was characterized in Fig. 4(c). Finally, it was understood from the simulations in Fig. 3 that the total length of the modulator would have a significant impact on the transmittance of the device, and therefore in order to further optimize the performance, the length of the periodic elements was varied, without changing the number or composition of the units. The results for this are shown in Fig. 4(d).

The periodic unit length (L_R), the length of the VO_2 segment in the periodic element (L_{VO2}), and the length of the Au segment in the periodic element (L_{Au}) are illustrated in Fig. 4(a). Fig. 4(b) shows that dependence of the transmittance and reflectance of a modulator formed of a single 100 nm periodic element on the percentage of gold (as compared to VO_2) in the periodic element. It was found that for a periodic element composed of 85% gold, the ER ratio of the modulator was maximized. In addition to this conclusion, however, an unexpected result was found. Despite the metallic VO_2 mode being more lossy than the Au mode, the transmission of the metallic VO_2 mode decreases as the portion of Au in the periodic unit increases. This can be explained by two phenomena. First, the metallic VO_2 index is very close to the Si waveguide index whereas the Au effective index is much larger, and therefore as the portion of Au in the periodic unit increases, the effective index of the periodic element as a whole becomes larger and the back reflection from the Si-modulator interface increases. Second, the plasmonic mode of the Au coated portion of the modulator actually helps to concentrate the light in the VO_2 and enhance the absorption. This can

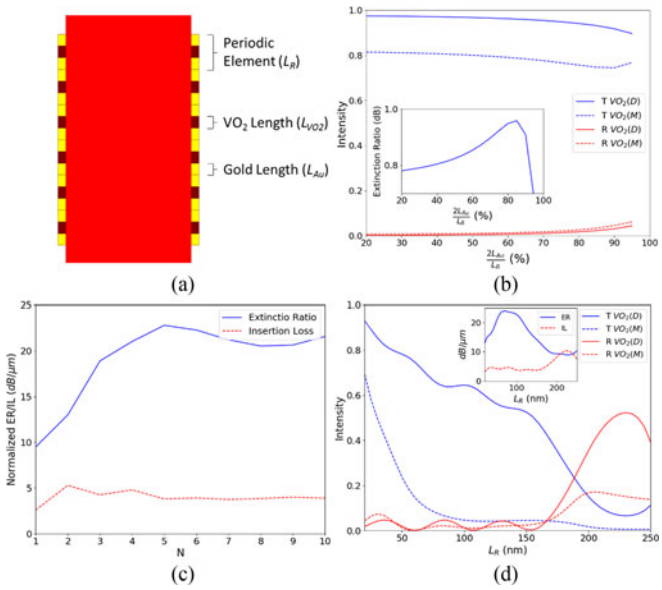

Fig. 4. Optimization of the 2D modulator structure. (a) Illustration of the modulator structure, showing the definition of one periodic element, the gold length and the VO2 length. (b) Change in the transmittance and reflectance of the modulator as the percentage of gold in a 100 nm long single periodic element modulator is changed. The inset of (b) shows the extinction ratio for the single unit modulator. (c) Extinction Ratio and Insertion Loss for modulators with a periodic element length of 100 nm, a periodic element that is 80% (80 nm gold, with 20 nm VO2) gold, and a varying number of periodic elements. (d) Transmittance and reflectance for a five periodic element modulator with 80% gold periodic elements, and a varying periodic elements length, with the inset shown the corresponding ER and IL.

clearly be seen in Fig. 1(c), where the pointing vector magnitude is evidently much stronger in the VO_2 regions than the other regions of the modulator.

Following the optimization of the Au/VO_2 ratio, the number of periodic units in the modulator was optimized. Although periodic element with 85% Au were found to be the ideal choice, for the periodic unit optimization and all further steps, a ratio of 80% was used. This was done to prevent the VO_2 length from being excessively short and impractical for fabrication. From Fig. 4(c) it can be seen that a modulator composed of five, 100 nm long, periodic units is ideal for obtaining an optimal ER per unit length.

The final parameter optimized was the length of the periodic units, denoted as L_R. The periodic element length was swept from 20 nm to 250 nm, and the transmittance and reflectance of the modulator in the metallic and dielectric VO_2 states were determined. In both the dielectric and metallic VO_2 state, there is an overall decrease in the transmittance as the periodic element length increases. This is simply a result of the increasing length of the lossy waveguide. In the dielectric VO_2 state, however, there is additionally a periodic oscillation to the transmittance and reflectance of the modulator. This can be attributed to the resonant length effect described in Section 3.1, the effective index of the modulator can be approximated as a weighted average [23] of the dielectric VO_2 coated and Au coated waveguide indices, $(0.8n_{Au} + 0.2n_{VO2} = 3.867 + 0.0858j)$. Based on this index, and the fact there are 5 periodic elements, we expect reflectance peaks to be separated by a difference in L_R of 40.1 nm. In Fig. 4(d), the separation between reflectance peaks is 45 $\pm$ 10 nm, which supports this conclusion. By taking advantage of this resonance, at an optimized length of 70 nm for the periodic elements, it was possible to obtain an ER of 23.98 dB/μm. The insertion loss (IL), which is simply the transmittance of the on state converted to a dB scale, was also exceptionally low at 1.6 dB (4.56 dB/μm). The high amplitude reflectance peak seen at a periodic unit length of 230 nm is a result of the periodic unit no longer being sub-wavelength in

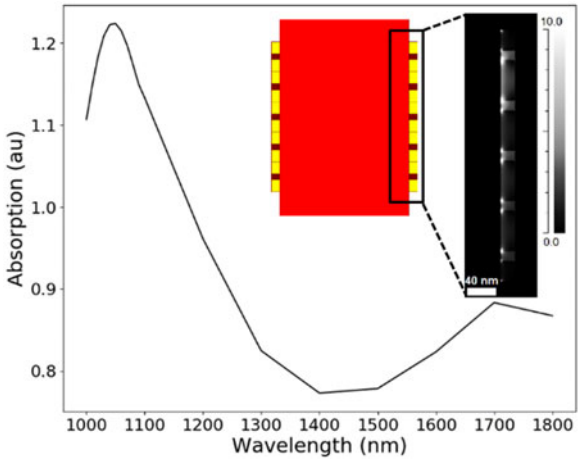

Fig. 5. Pump light wavelength optimization. (a) Total absorption of a pump light in VO_2 as a function of pump wavelength. (b) Absorption distribution in the modulatorfor a pump wavelength of 1064 nm.

size. At this point, each periodic unit is on the order of a wavelength in length, and the modulator behaves as a Bragg reflector.

3.3 Pump Light Wavelength

As a final step to the optimization of the 2D waveguide modulator, a pump light wavelength had to be chosen. Recent theoretical work suggests that the optically induced VO_2 phase transition is caused by a critical density of photo-excited carriers in the VO_2 causing an instantaneous collapse of the VO_2 bandgap, and the onset of metallic behavior [16]. Based on this, the absorption of the pump light in the VO_2 region was used as a metric for determining the ideal pump light wavelength. It was also predicted that because the Au/VO_2 nanostructure consists of many metal-dielectric-metal nanogaps, there should be a resonant wavelength for which light is coupled strongly to this cavity. In order to find this wavelength, the optimized modulator was excited by a varying wavelength, and the absorption in the VO_2 was monitored [see Fig. 5(a)]. For a pump light wavelength of 1050 nm, an absorption peak was observed. A pump wavelength of 1064 nm was chosen due to the ready availability of this wavelength. The spatial distribution of the absorption for a 1064 nm pump light is shown in Fig. 5(b).

3.4 3-D Modulator

Using the same optimization process used for the 2D slab modulator, the periodic element length, number of periodic elements and periodic element composition of a 3D modulator [see Fig. 1(a)] were optimized. In this design, the Si waveguide height and width were kept at 300 nm and 320 nm respectively. After optimization, ideal number of periodic elements, and Au/VO_2 ratio was found to be the same as for the 2D modulator (5 and 80% Au). However, after optimizing the periodic element length [see Fig. 6(a)], an optimal length of 110 nm was found, for which an ER of 26.85 dB/μm, with an IL of only 7.17 dB (13.04 dB/μm), was obtained. When the VO_2 is in its dielectric state, the modulator has a transmittance at 1550 nm of 19.22%, which is changed to 0.64% when the VO_2 is in its metallic state. With a total device length of only 550 nm, this device is comparable to other modulators in the literature [4], [18], [31], [32], [33] and has the added benefit of being optically pumped. In Fig. 6(b) and (c), the Poynting vector magnitude of 1550 nm light propagating through a horizontal cross section at the center of the modulator when the VO_2 is in its dielectric state [see Fig. 6(b)] and metallic state [see Fig. 6(c)] is shown. The focusing of the signal light into the metallic VO_2 is evident by the strong Poynting vector magnitude in the vicinity of the metallic VO_2. The inset

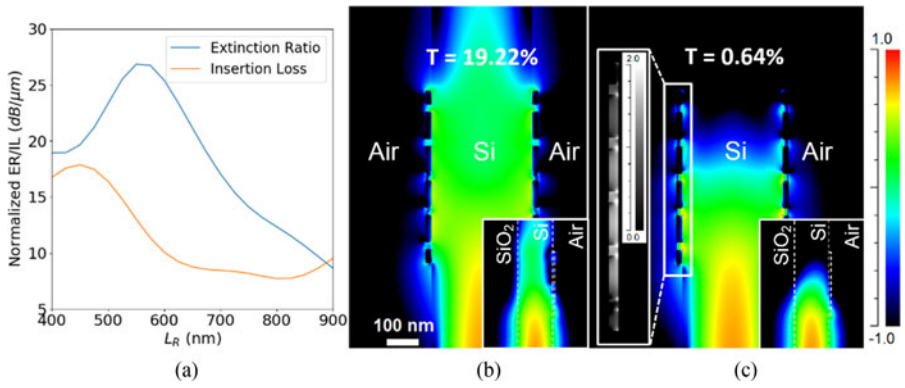

Fig. 6. 3D modulator performance. (a) ER and IL in dB/μm as a function of periodic element length. At the optimal length of 110 nm, ER of 26.85 dB/μm is achieved. The log scale Poynting vector magnitude for a horizontal cross section through the middle of the Si waveguide is shown in (b) for the dielectric VO_2 state and (c) for the metallic VO_2 state. Insets in the bottom right of (b) and (c) show the Poynting vector magnitude in a vertical cross through the center of the waveguide. The inset on the left in (c) shows the absorption distribution on the left of the horizontal cross-section of the modulator for a 1064 nm pump light.

of Fig. 6(c), where the absorption on one side of the modulator is shown, additionally demonstrates that a pump light at 1064 nm is strongly absorbed in the VO_2 and therefore can be used to induce the metal-insulator transition in the VO_2 through the generation of photo-excited carriers.

4. Conclusion

In this work, a 2D slab waveguide and a 3D ridge waveguide hybrid photonic-plasmonic all-optical modulator were designed and optimized. Through an in-depth study of the 2D slab waveguide modulator, it was determined that the key factors affecting the performance of the modulators were the ratio of the Au/VO_2 segment length, the number of Au/VO_2 periodic elements in the modulators, and the total length of the modulators. By optimizing these three parameters, a 3D modulator design with an ER of 26.85 dB/μm and an IL of only 7.17 dB was achieved. The design was also found to efficiently concentrate pump light at 1064 nm into the VO_2 regions, thus enabling an optically induced metal-insulator transition in the VO_2. This design can be microfabricated, and future work will focus on the experimental demonstration of this waveguide integrated all-optical modulator.

References

[1] G. T. Reed, G. Mashanovich, F. Y. Gardes, and D. J. Thomson, "Silicon optical modulators," *Nat. Photon.*, vol. 4, no. 8, pp. 518–526, 2010.
[2] G. T. Reed *et al.*, "Recent breakthroughs in carrier depletion based silicon optical modulators," *Nanophotonics*, vol. 3, no. 4/5, pp. 229–245, 2014.
[3] W. Li *et al.*, "Ultrafast all-optical graphene modulator," *Nano Lett.*, vol. 14, no. 2, pp. 955–959, 2014.
[4] A. Joushaghani, B. A. Kruger, S. Paradis, D. Alain, J. Stewart Aitchison, and J. K. S. Poon, "Sub-volt broadband hybrid plasmonic-vanadium dioxide switches," *Appl. Phys. Lett.*, vol. 102, no. 6, 2013, Art. no. 061101.
[5] J. D. Ryckman *et al.*, "Photothermal optical modulation of ultra-compact hybrid Si-VO2 ring resonators," *Opt. Exp.*, vol. 20, no. 12, 2012, Art. no. 13215.
[6] A. Joushaghani, J. Jeong, S. Paradis, D. Alain, J. Stewart Aitchison, and J. K. S. Poon, "Wavelength-size hybrid Si-VO_2 waveguide electroabsorption optical switches and photodetectors," *Opt. Exp.*, vol. 23, no. 3, pp. 3657–3668, 2015.
[7] L. D. S. Diana, F. C. Juan, A. R. Escutia, and P. S. Kilders, "Ultra-compact electro-absorption VO_2–Si modulator with TM to TE conversion," *J. Opt.*, vol. 19, no. 3, 2017, Art. no. 035401.
[8] J. T. Kim, "CMOS-compatible hybrid plasmonic modulator based on vanadium dioxide insulator-metal phase transition," *Opt. Lett.*, vol. 39, no. 13, pp. 3997–4000, 2014.
[9] D. Tanaka *et al.*, "Ultra-small, self-holding, optical gate switch using Ge2Sb2Te5 with a multi-mode Si waveguide," *Change*, vol. 20, no. 9, pp. 442–445, 2012.

[10] M. Rude *et al.*, "Optical switching at 1.55 μm in silicon racetrack resonators using phase change materials," *Appl. Phys. Lett.*, vol. 103, no. 14, 2013, Art. no. 141119.
[11] M. Stegmaier, C. RÍos, H. Bhaskaran, and W. H. P. Pernice, "Thermo-optical effect in phase-change nanophotonics," *ACS Photon.*, vol. 3, no. 5, pp. 828–835, 2016.
[12] Z. Yang, C. Ko, and S. Ramanathan, "Oxide electronics utilizing ultrafast metal-insulator transitions," *Annu. Rev. Mater. Res.*, vol. 41, no. 1, pp. 337–367, 2011.
[13] G. Stefanovich, A. Pergament, and D. Stefanovich, "Electrical switching and Mott transition in VO_2," *J. Phys. Condens. Matter*, vol. 12, no. 41, pp. 8837–8845, 2000.
[14] M. Liu *et al.*, "Terahertz-field-induced insulator-to-metal transition in vanadium dioxide metamaterial," *Nature*, vol. 487, no. 7407, pp. 345–348, 2012.
[15] K. Appavoo *et al.*, "Ultrafast phase transition via catastrophic phonon collapse driven by plasmonic hot-electron injection," *Nano Lett.*, vol. 14, no. 3, pp. 1127–1133, 2014.
[16] D. Wegkamp and J. Stähler, "Ultrafast dynamics during the photoinduced phase transition in VO2," *Prog. Surf. Sci.*, vol. 90, no. 4, pp. 464–502, 2015.
[17] A. Joushaghani, J. Jeong, S. Paradis, D. Alain, J. Stewart Aitchison, and J. K. S. Poon, "Voltage-controlled switching and thermal effects in VO_2 nano-gap junctions," *Appl. Phys. Lett.*, vol. 104, no. 22, pp. 2012–2016, 2014.
[18] P. Markov, K. Appavoo, R. F. Haglund, and S. M. Weiss, "Hybrid Si-VO2-Au optical modulator based on near-field plasmonic coupling," *Opt. Exp.*, vol. 23, no. 5, pp. 6878–6887, 2015.
[19] W. L. Barnes, A. Dereux, and T. W. Ebbesen, "Surface plasmon subwavelength optics," *Nature*, vol. 424, no. 6950, pp. 824–830, 2003.
[20] M. Kauranen and A. V. Zayats, "Nonlinear plasmonics," *Nat. Photon.*, vol. 6, pp. 329–347, 2012.
[21] M. E. Stewart *et al.*, "Nanostructured plasmonic sensors," *Chem. Rev.*, vol. 108, no. 2, pp. 494–521, 2008.
[22] O. L. Muskens *et al.*, "Antenna-assisted picosecond control of nanoscale phase- transition in vanadium dioxide," *Light Sci. Appl.*, vol. 5, no. 10, pp. 1–25, 2016.
[23] P. J. Bock *et al.*, "Subwavelength grating periodic structures in silicon-on-insulator: A new type of microphotonic waveguide.," *Opt. Exp.*, vol. 18, no. 19, pp. 20251–20262, 2010.
[24] N. F. Brady *et al.*, "Heterogeneous nucleation and growth dynamics in the light-induced phase transition in vanadium dioxide," *J. Phys. Condens. Matter*, vol. 28, no. 12, 2016, Art. no. 125603.
[25] Y. L. Ho, L. C. Huang, and J. J. Delaunay, "Spectrally selective photocapacitance modulation in plasmonic nanochannels for infrared imaging," *Nano Lett.*, vol. 16, no. 5, pp. 3094–3100, 2016.
[26] H. Matsui, Y. L. Ho, T. Kanki, H. Tanaka, J. J. Delaunay, and H. Tabata, "Mid-infrared plasmonic resonances in 2D VO_2 nanosquare arrays," *Adv. Opt. Mater.*, vol. 3, pp. 1759–1767, 2015.
[27] A. D. Rakic, A. B. Djurisic, J. M. Elazar, and M. L. Majewski, "Optical properties of metallic films for vertical-cavity optoelectronic devices," *Appl. Opt.*, vol. 37, no. 22, pp. 5271–5283, 1998.
[28] E. D. Palik, *Handbook of Optical Constants of Solids*. San Diego, CA, USA: Academic, 1998, vol. 3.
[29] I. H. Malitson, "Interspecimen comparison of the refractive index of fused silica," *J. Opt. Soc. Amer.*, vol. 55, no. 10, pp. 1205–1209, 1965.
[30] P. Berini, "Long-range surface plasmon polaritons," *Adv. Opt. Photon.*, vol. 1, no. 3, pp. 484–588, 2009.
[31] R. M. Briggs, I. M. Pryce, and H. A. Atwater, "Compact silicon photonic waveguide modulator based on the vanadium dioxide metal-insulator phase transition.," *Opt. Exp.*, vol. 18, no. 11, pp. 11192–11201, 2010.
[32] J. D. Ryckman, K. A. Hallman, R. E. Marvel, R. F. Haglund, and S. M. Weiss, "Ultra-compact silicon photonic devices reconfigured by an optically induced semiconductor-to-metal transition," *Opt. Exp.*, vol. 21, no. 9, pp. 10753–10763, 2013.
[33] K. J. Miller, K. A. Hallman, R. F. Haglund, and S. M. Weiss, "Silicon waveguide optical switch with embedded phase change material," *Opt. Exp.*, vol. 25, no. 22, pp. 26527–26536, 2017.